Available online at www.sciencedirect.com
ScienceDirect
Journal of Power Sources 180 (2008) 84–91
JOURNAL OF POWER SOURCES
www.elsevier.com/locate/jpowsour

Electrochemically synthesized Cu/Pt core-shell catalysts on a porous carbon electrode for polymer electrolyte membrane fuel cells

Z.D. Wei [a,b,*], Y.C. Feng [b], L. Li [b,c], M.J. Liao [b], Y. Fu [b], C.X. Sun [a], Z.G. Shao [d], P.K. Shen [e,**]

[a] *The State Key Laboratory of Power Transmission Equipment & System Security and New Technology, Chongqing University, Chongqing 400044, China*
[b] *School of Chemistry and Chemical Engineering, Chongqing University, Chongqing 400044, China*
[c] *School of Material Science and Engineering, Chongqing University, Chongqing 400044, China*
[d] *Dalian Institute of Chemical Physics, Chinese Academy of Sciences, Dalian 116023, China*
[e] *The State Key Laboratory of Optoelectronic Materials and Technologies, School of Physics and Engineering, Sun Yat-Sen University, Guangzhou 510275, China*

Received 27 January 2008; accepted 30 January 2008
Available online 14 February 2008

Abstract

A novel two-step method has been developed to efficiently prepare Cu/Pt core-shell structured catalysts for the first time. The Cu is first electrodeposited on the surface of the porous carbon electrode (PCE) and the deposited Cu is then partially replaced by Pt spontaneously. The addition of the thiourea (TU) along with the pH adjustment can tremendously reduce the self-dissolution of Cu due to dissolved oxygen. The results show that Cu/Pt core-shell structured catalysts display very good activities even at very low Pt loadings. The peak power density of a single cell using Cu/Pt core-shell structured catalysts is over 0.9 W cm^{-2} at Pt loadings as low as 0.24 mg cm^{-2} on each cathode and anode. This study shows that it is possible to apply this method for fabrication various core-shell structured functional materials.

Keywords: Core-shell catalyst; PEMFC; Electrodeposition; Electrocatalysis; Platinum

1. Introduction

Polymer electrolyte membrane fuel cells (PEMFCs) using hydrogen as the fuel have been recognized as a potential power source for zero-emission vehicles. However, to become commercially viable, PEMFCs have to overcome the barrier of high catalyst cost [1] among others. Both lowering loadings of noble metal catalysts and improving their utilization are the keys to the success of PEMFCs commercialization. Conventional methods employed for fabricating the membrane–electrode-assembly (MEA) of PEMFC includes painting, spraying or printing of catalyst ink that contains binder and carbon supported catalyst onto the gas diffusion layer or electrolyte membrane [2,3]. Owing to the agglomeration of Pt/C powders, Pt particles are not always in direct contact with the solid electrolyte phase like Nafion (DuPont, USA). In other words, the Pt catalyst is not utilized effectively. The active electrocatalyst sites should not only accessible to the reactants in the fuel cell but also electronically connected to the current collectors along with the ionically connected to the electrolyte.

Much effort has been placed on development of electrodes with high utilization of noble metal catalysts by using the ordered nanoporous arrays of carbon [4], improving method in preparation of catalyst ink [5], sputtering metal catalyst directly onto the surface of Nafion-bonded carbon paper [6], and electrodepositing metal catalyst on porous substrates [7–9], etc.

* Corresponding author at: School of Chemistry and Chemical Engineering, Chongqing University, Chongqing 400044,China. Tel.: +86 23 65106253; fax: +86 23 65112822.
** Corresponding author.
E-mail addresses: zdwei@cqu.edu.cn (Z.D. Wei), fengyongchao8@sohu.com (Y.C. Feng), liliracial@126.com (L. Li), windy511@sina.com (M.J. Liao), fuying_1981@163.com (Y. Fu), zhgshao@dicp.ac.cn (Z.G. Shao), stsspk@mail.sysu.edu.cn (P.K. Shen).

0378-7753/$ – see front matter © 2008 Elsevier B.V. All rights reserved.
doi:10.1016/j.jpowsour.2008.01.086

Recently, Tian et al. [10] reported that Pt nanocrystals with an unusual tetrahexahedral shape could be obtained by an electrochemical square-wave potential treatment of electrodeposited Pt nanospheres supported on a smooth glassy carbon electrode. The single tetrahexahedral nanocrystals exhibit enhanced (up to 400%) catalytic activity per unit surface area for electrooxidation of small organic fuels such as formic acid and ethanol. However, for catalytic activity per unit mass of Pt, the overall activity of these larger tetrahexahedral Pt nanocrystals is less than that of the 3-nm commercial Pt nanoparticles. Meanwhile this excellent work did not involve how to prepare the Pt nanoparticles efficiently on a porous substrate.

Electrodeposition of noble metal catalysts on a porous carbon electrode (PCE) in an aqueous solution opens a promising way in increasing utilization of metal catalysts practically. Pulse current, direct current and cyclic voltammetry have been employed to deposit Pt onto a PCE for anodes and cathodes of H_2-feed PEMFCs. Electrodeposition in an aqueous bath can selectively deposit platinum catalysts only onto the electrode regions, where ions and electrons are accessible because only in those regions there are electron transport channels and metal ion transport channels. However, during the Pt electrodeposition, Pt prefers to deposit on the surface of Pt particles that are already existed, which leads to a larger size of deposited Pt particles, especially, in the case of higher Pt loadings. Usually, the sizes of Pt particles electrochemically deposited fall in the range of 20–70 nm [7–13], unless the Pt loading is ultra-low, for example, 0.05 mg cm^{-2} [14]. It would be no advantage for a catalyst with Pt particle size of 20–70 nm even though every Pt particle was fully utilized since the widely used commercial Pt/C catalysts (e.g. Johnson-Matthey Co.) are only ca. 2–4 nm. In addition, the current efficiency for Pt electrodeposition is extremely low in a simple acidic aqueous solution, in which the hydrogen evolution is unavoidable [15]. The current efficiency for Pt electrodeposition on the porous carbon electrode (PCE) will be further reduced since the hydrogen evolution is sped up by the Pt particles. The hydrogen bubbles formed on the Pt/PCE may block the transportation of the deposition solution, consequently interrupts the deposition process. Serious hydrogen evolution may not only damage the structure of the PCE, but also causes the increase in local pH value, which may further lead to hydrolysis of Pt salts. Thus it is a challenge to achieve smaller electrodeposited Pt particles and reduced hydrogen evolution reaction (HER) in electrodeposition.

The direct deposition of Pt on the PCE is not feasible for the preparation of catalytic electrode because of the good catalytic activity of Pt in the HER. Therefore, the searching for a metal, which has a high overpotential to the HER, almost 100% current efficiency of electrodeposition in an aqueous solution, and can be easily replaced afterward by Pt in a Pt salt solution, becomes the key to this problem. We found that copper meets almost all the requirements mentioned above. In this study, the Cu nanoparticles were initially electrochemically deposited on the PCE to form a Cu/PCE electrode. Compared to Pt electrodeposition, the current efficiency of copper electrodeposition is as high as 95%. The bath of copper deposition has a very good throw power and deep deposition capability (it means that Cu can be well deposited on the inner pore surface of the PCE). The top surface of Cu deposits was then replaced by Pt by dipping a Cu/PCE electrode in a Pt salt solution and finally formed a Cu/Pt core-shell-like nanoparticles supported on the PCE.

The high surface-area-to-volume ratio of the core-shell nanoparticles would make them more active. For example, Au/Pt core-shell catalyst prepared by successive reduction of $HAuCl_4$ and H_2PtCl_6 precursors displays good electrocatalytic activity for electrocatalytic reduction of oxygen to water [16]. Cu/Pt core-shell catalyst prepared by polyol reduction has greater selectivity for N_2 formation [17]. Au/PS250-b-PAA13 core-shell catalyst prepared by self-assembly has the alterable optical properties via variation of the composition of the copolymer shell [18]. Penner's group prepared Ag/Cu core-shell particles by electrodepositing silver particles first and then electrodepositing copper on freshly cleaved highly oriented pyrolytic graphite [19]. Although core-shell catalysts have been extensively studied, the deposition of Cu on a porous carbon electrode to form Cu/Pt core-shell catalyst for application in PEMFC has not been reported.

2. Experimental

2.1. Preparation of a porous carbon electrode

The PCE was prepared in the same way as described previously [14,15]. In brief, the PCE consists of two different carbon layers—hydrophobic and hydrophilic. Firstly, carbon paper (Tony Co., Japan.) was dipped in 30% PTFE solution for 30 min, dried in the air and sintered at 340 °C for 30 min The ink-containing carbon powder (Vulcan XC-72, Cabot Co., USA) and 10% PTFE (the dry weight ratio of PTFE to carbon powder was kept at 1:4) in isopropyl alcohol was coated on the PTFE treated carbon paper and then dried at 340 °C to form hydrophobic layer. Subsequently, Vulcan XC-72 carbon powders were treated in nitric acid at refluxing condition for 2 h and mixed with 5% Nafion in isopropyl alcohol to form the hydrophilic ink. It was spread on the top of the hydrophobic layer. Finally, the PCE was obtained after dried at 145 °C for 20 min.

2.2. Formation of Cu cores by electrodeposition

The electrodeposition of Cu was carried out in a three-electrode cell. The PCE was employed as a working electrode and a piece of copper with 2.5 cm × 6 cm as a counter electrode. A saturated Ag/AgCl electrode (SSCE) was employed as a reference electrode. The electrodeposition of copper was performed on the PCE in an acidic copper sulfate bath consisting of 0.25 M $CuSO_4 \cdot 5H_2O$ and 2 M H_2SO_4 at 25 °C. Rectangular galvanostatic pulses modulated by changing peak current densities, current pulse frequency were applied to deposit copper. The electrodeposition was performed on Autolab Potentiostat/galvanostat PGSTAT 30. Dual-pulse current (DPC) was adopted to deposit Cu cores. DPC is based on an extremely short nucleation pulse of high cathodic polarization followed

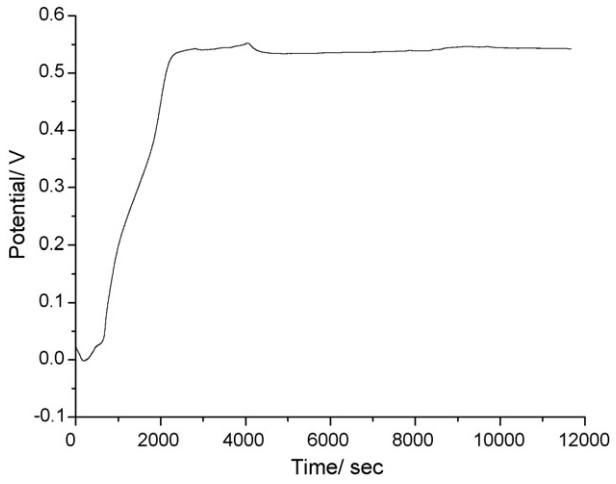

Fig. 1. The open-circuit potential (Eocp) of the electrode in contact with the 0.5 g L^{-1} H_2PtCl_6 solution.

by a slightly longer growth pulse at low cathodic overpotential. The ideal situation is where nucleation occurs only in the first pulse and crystalline growth in the second pulse [20,21]. Tailor-made nanoparticle structures with respect to size, density and monodispersity are obtained if the pulse parameters are carefully chosen and adjusted.

2.3. Formation of Pt monolayer shell by replacement of the Cu

The PCE loaded with Cu particles was dipped into a bath containing 0.5 g L^{-1} H_2PtCl_6 and 3 g L^{-1} HCl solution in order to form Pt shells by replacement. To avoid the oxidation of Cu nanoparticles by dissolved oxygen, nitrogen was bubbled during the replacement. The replacement was judged by the open circuit potential of the PCE during replacement as illustrated in Fig. 1. The replacement is completed when the PCE potential remains unchanged.

2.4. Preparation of comparison electrodes

Two electrodes made from direct electrodeposition of Pt on the PCE and from the commercial 40% Pt/C catalysts (Jonhson-Matthey), respectively, were used for comparison. The electrodeposition of platinum was performed on the PCE in a bath containing 10 g L^{-1} of H_2PtCl_6 and 60 g L^{-1} of HCl at 65 °C. Rectangular galvanostatic pulses modulated by changing peak current densities, current pulse frequency were applied to deposit Pt. The commercial catalyst electrode was fabricated using 40% Pt/C instead of the Vulcan XC-72 carbon in the hydrophilic ink of the PCE as described in Section 2.1.

2.5. Characterization of the electrodes

The performance of the prepared electrode for catalysis of the ORR was assessed by linear-sweep voltammetry at a sweep rate of 2 mV s^{-1} in O_2 saturated 0.5 M H_2SO_4 solution at room temperature (25 ± 2 °C). The experiment was performed using a conventional three-electrode cell. The prepared electrodes were used as the working electrode. The platinum wire was employed as the counter electrode. All potential was relative to the SSCE unless otherwise stated.

The field emission scanning electron microscope (FESEM) (FEI Nova 400, Peabody, MA) was utilized to observe surface morphologies of the electrodes. The atomic ratios of the Cu/Pt catalysts were determined by energy dispersive X-ray spectroscopy (EDX) attached to the FESEM equipment. A spectrophotometer (TU-1900/TU-1901, Beijing Puxi, China) was used to determine the Pt content in an electrode according to the method described in reference [22].

2.6. Single cell test

The membrane–electrode assembly (MEA) was fabricated by hot pressing a sandwich structured Cu/Pt electrode, Nafion® 112 membranes (DuPont, USA) and another Cu/Pt electrode

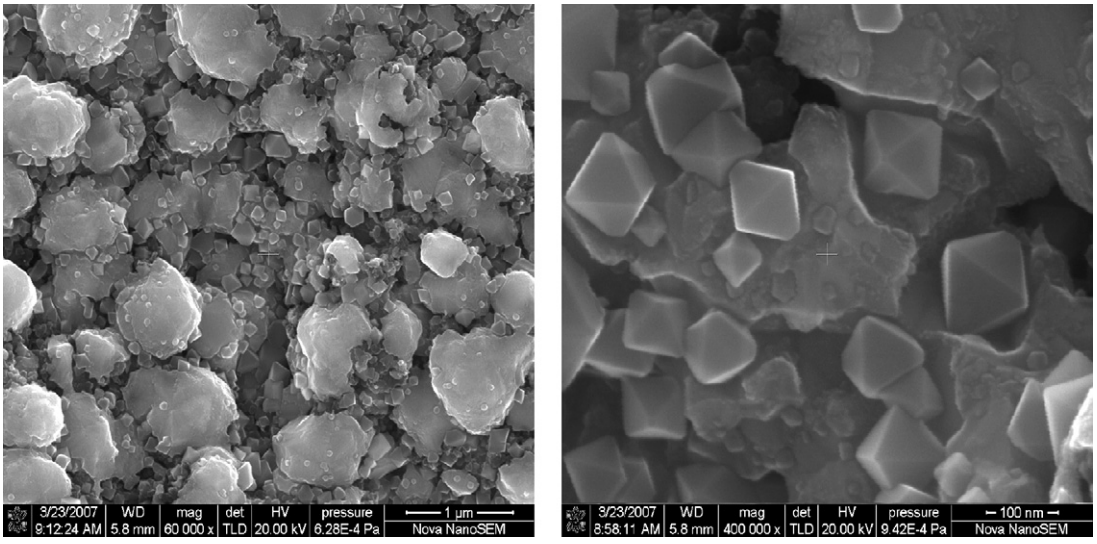

Fig. 2. SEM micrographs of copper nanoparticles electrodeposited on the PCE.

in series at 137 °C and 6 MPa for 3 min. Nafion® 112 membranes were pretreated with 3 vol.% H_2O_2 and 0.5 M H_2SO_4 for 1 h to remove impurities, respectively. The membranes were then washed several times in hot ultra-pure water. The performance of the MEA was tested on a Fuel Cell Test Station (Fuel Cell Technologies Inc., USA). The pure hydrogen and oxygen were fed as the fuel and the oxidant, respectively. The operating temperature of the cell was 70 °C. Backpressures of the anode and cathode were kept at 200 kPa (absolute pressure). Before each experiment was conducted, nitrogen was used to purge the residual fuel and oxidant in the cell and pipelines.

3. Results and discussion

Fig. 2 shows that Cu nanoparticles with an octahedron shape and an average diameter of about 80–90 nm have been successfully deposited on the PCE. The Cu nanoparticles were highly dispersed throughout the whole PCE including the inner sites of the PCE.

Theoretically, it is possible for the following reaction to take place spontaneously

$$2Cu + PtCl_6^{2-} = Pt + 2Cu^{2+} + 6Cl^- \quad (1)$$

Platinum complexes and chloride ions have the following equilibrium and corresponding Nernst potential

$$PtCl_6^{2-} + 2e = PtCl_4^{2-} + 2Cl^- \quad 0.72\,V vs.SHE \quad (2)$$

While Cu and Cu^{2+} have the following equilibrium in an acidic solution and the corresponding Nernst potential

$$Cu^{2+} + 2e = Cu \quad 0.34\,V vs.SHE \quad (3)$$

Thus, it is likely for reaction (1) to take place spontaneously. Fig. 1 shows the time history the open-circuit potential (Eocp) of the PCE loaded with Cu when it was in contact with solution of 0.5 g L^{-1} H_2PtCl_6 and 3 g L^{-1} HCl. The time dependence of Eocp indicates that platinum replacement completed in 3000 s.

Fig. 3 shows the CVs of a Pt wire electrode in 3 g L^{-1} HCl with and without TU, in which the PCE loaded with Cu were in advance dipped in for a period of time. The reduction and oxidation peaks in line 1 of Fig. 3 correspond to the reduction of dissolved Cu^{2+} and oxidation of reduced Cu, respectively. The situation is completely changed in the case of 3 g L^{-1} HCl-containing TU as illustrated by line 2 of Fig. 3. It indicates that the TU can inhibit the dissolution of deposited Cu and thus guarantee that the deposited Cu is only react with Pt ions.

Fig. 4 shows SEM micrographs of Pt nanoparticles prepared by the pathway of Cu/Pt and TEM images of Pt nanoparticles by direct electrodeposition of Pt. It should be noted that SEM

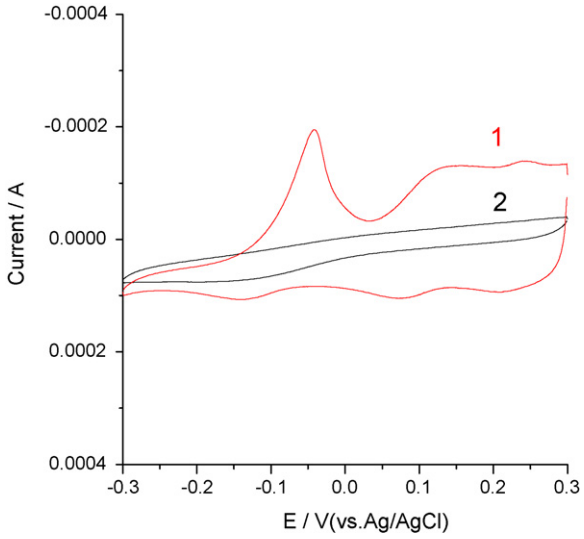

Fig. 3. CVs of Pt electrode in 3 g L^{-1} HCl without TU (line 1) and with TU (line 2), in which the PCE loaded Cu were dipped in advance.

micrographs of Pt nanoparticles reflect the genuine dispersion of Pt particles on the PCE, but the TEM images only reflect the Pt particle size but not its genuine dispersion on the PCE because the TEM images were obtained by an indirect rather than direct observation to the deposited Pt on the PCE. The electrodeposited Pt particle together with the carbon carrier and Nafion polymer was first scratched off from the PCE and ultrasonically suspending in isopropyl alcohol, and then observed on PHILIPS TECNAI 10 transmission electron microscope. Regardless of high or low loadings of Pt, the Pt particle size and dispersion on the PCE via the pathway of Cu/Pt always keep a very ideal status. However, the Pt particle size in the case of direct electrodepositing Pt will become intolerably large with increased Pt loadings. The catalytic behavior for the ORR of the electrodes (A–D) in Fig. 4 is demonstrated in Fig. 5. It is not strange that the electrode (B), which has a small Pt size, good Pt dispersion and proper Pt loadings, exhibits the best catalytic behavior for the ORR.

To prevent the deposited nano-copper from reacting with the dissolved oxygen in solution of H_2PtCl_6 and HCl, thiourea (TU) was used as an inhibitor. Table 1 presents the Cu/Pt atomic ratios in Cu/Pt nanoparticles as the replacement solution was adjusted by TU and pH value. The atomic ratios of copper to platinum in Cu/Pt nanoparticles increase with the addition of TU and pH value. As a matter of fact, the replaced Pt catalysts would be close to a solid Pt sphere if the pH and/or inhibitor were not adjusted and/or added. The Cu/Pt core-shell structure nanoparticles were confirmed by images of SEM and EDX presented in Figs. 6 and 7, respectively. The ultrafine and uniformly

Table 1
Cu/Pt atomic ratios in Cu/Pt core-shell structured catalysts in different solutions with TU and different pH values

Electrode no.	E	F	G	H
Condition in displacement	pH < 1	pH = 6	pH < 1 plus 10 mg L^{-1} of TU	pH = 6 plus 10 mg L^{-1} of TU
Ratio of Cu/Pt	3.33/96.67	19.02/80.98	20.57/79.43	32.01/67.99
Pt loading (mg cm^{-2})	0.12	–	0.11	0.10

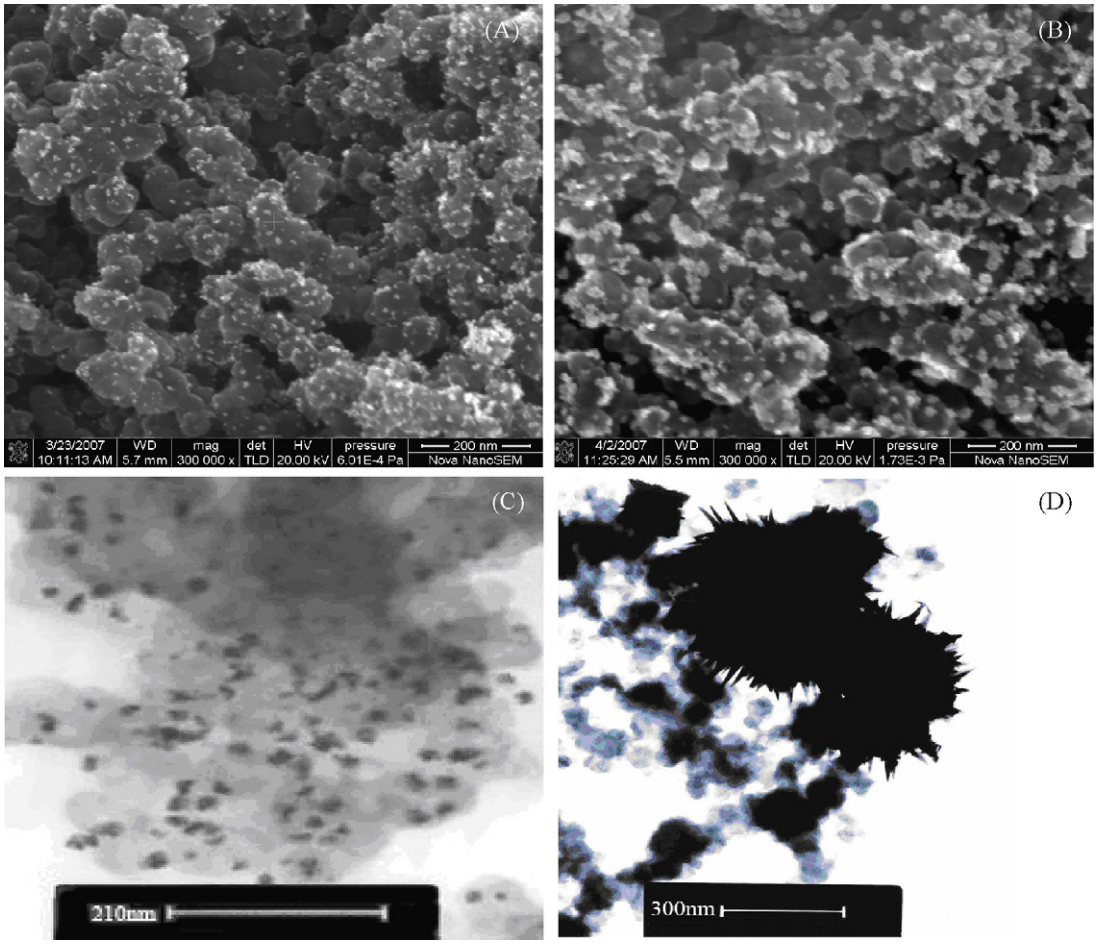

Fig. 4. SEM micrographs of Pt nanoparticles prepared by Cu/Pt (A and B) and TEM images of Pt nanoparticles by direct electrodeposition of Pt (C and D), where Pt loadings are 0.05 mg cm^{-2} and 0.30 mg cm^{-2}, (C) 0.23 mg cm^{-2} and 0.51 mg cm^{-2} for A–D, respectively.

dispersed Cu/Pt core-shell structure nanoparticles were clearly shown in Fig. 6. A locally magnified image of Cu/Pt core-shell-like structured nanoparticles (Fig. 6(d)) shows that a dark core is surrounded by a bright circle, where the dark image is ascribed to the element with low atomic number while the bright image to one with high atomic number [23], herein, the former corresponds to Cu and the latter Pt. The Cu/Pt core-shell structure is further confirmed by EDX elemental map images in Fig. 7, where two kinds of uniformly dispersed speckles correspond to Cu and Pt, respectively. Fig. 8 shows the catalytic performance for the ORR of the electrodes prepared according to the conditions listed in Table 1.

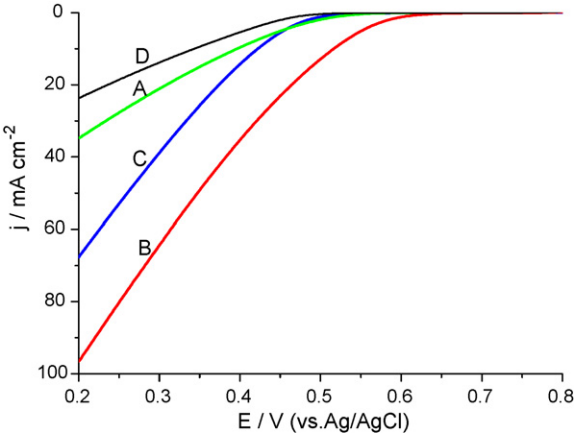

Fig. 5. Catalytic behavior for the ORR of the electrodes (A–D) in Fig. 4.

The comparison between the electrodes with Cu/Pt core-shell structured catalysts and commercial Pt/C catalyst is illustrated in Fig. 9. The compositions of the electrodes are exactly the same except the Pt loadings and the way of Pt loaded. The loadings of Cu/Pt core-shell structured catalysts and commercial 40% Pt/C catalyst on the electrode surface are 0.10, 0.30, and 0.27 mg cm^{-2}, respectively. Obviously, the catalytic activities of the electrodes with Cu/Pt core-shell structured catalysts are much higher than that of the commercial Pt/C solid sphere catalysts even though the Pt loadings in the case of Cu/Pt core-shell structured catalyst are lower (0.10 mg cm^{-2} against 0.27 mg cm^{-2}). The remarkably high activity for the ORR on the electrodes made from Cu/Pt core-shell structured catalysts is attributed to the high utilization of Pt and the high surface area. On the one hand, Pt particles in Cu/Pt core-shell structured catalysts are electrodeposited at the interface between the carbon powder and the Nafion electrolyte, while only part of the commercial Pt/C powders are exposed to the interface between the carbon powder and the Nafion electrolyte due to

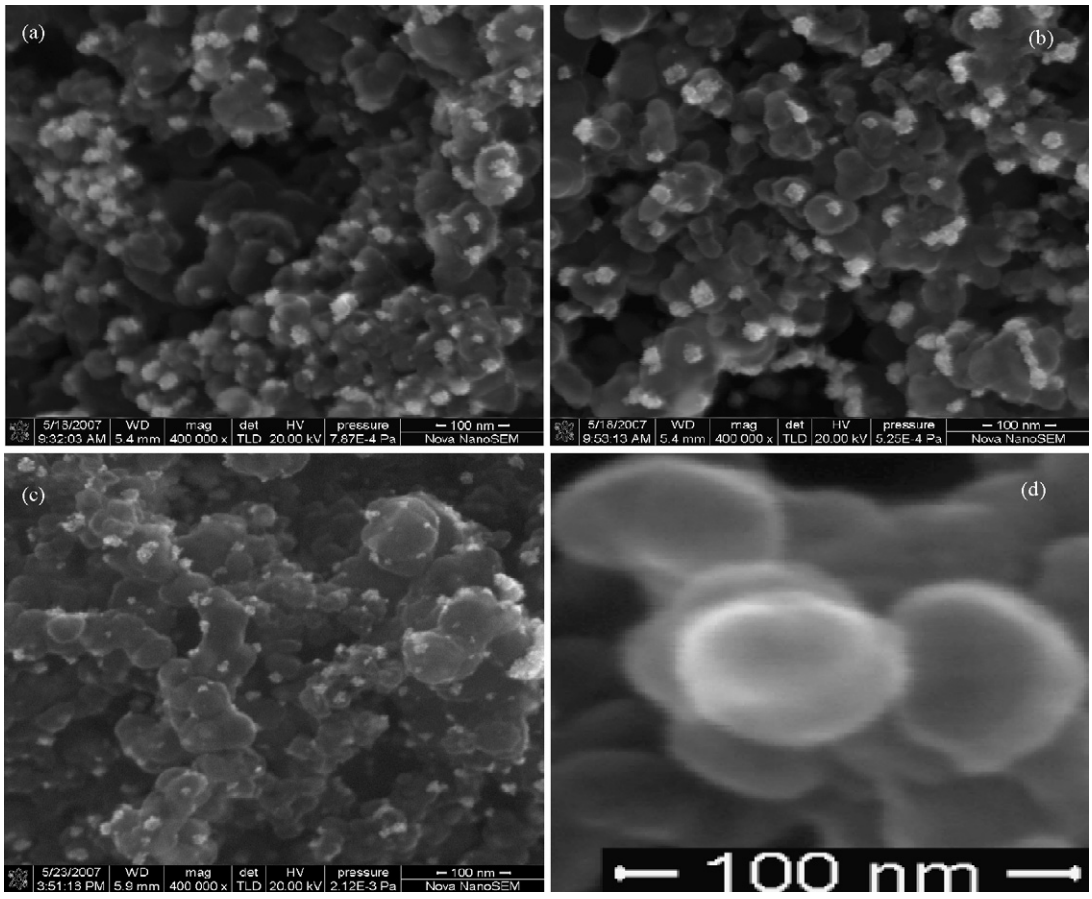

Fig. 6. SEM micrographs of the electrodes E (a), F (b) and H (c). (d): enlarged SEM micrograph of (c).

inevitable agglomeration. However, the catalysts with Cu/Pt core-shell structure can maximize the presence of Pt particles on the catalyst surface.

The stability of the Cu/Pt core-shell structured catalyst was determined according to a method adopted in literature [24]. The potential sweep was ranging from −0.2 to 1.2 V rather than from 0.6 to 1.1 V in literature [24]. The accelerated stability testing by continuously applying linear potential sweeps between −0.2 and 1.2 V was performed to the electrode with Cu/Pt core-shell structured catalyst. The change in the CV profile of the electrode after many cycles to assess the stability of the Pt catalysts in the electrode. Agglomeration derived from the re-deposition of dissolved Pt ions at low potential and dissolution of Pt particles at high potential would both lead to the Pt surface loss and thus cause the electrode's CV profile shrink. Fig. 10 shows the profile of the 10th and 100th CVs of the electrode with Cu/Pt core-shell structured catalysts in N_2 saturated 0.5 M H_2SO_4. The profiles of the 10th and 100th CVs are hardly changed, especially, in the hydrogen adsorption/desorption area, where the profile of the CV intrinsically reflects the Pt active surface area of the elec-

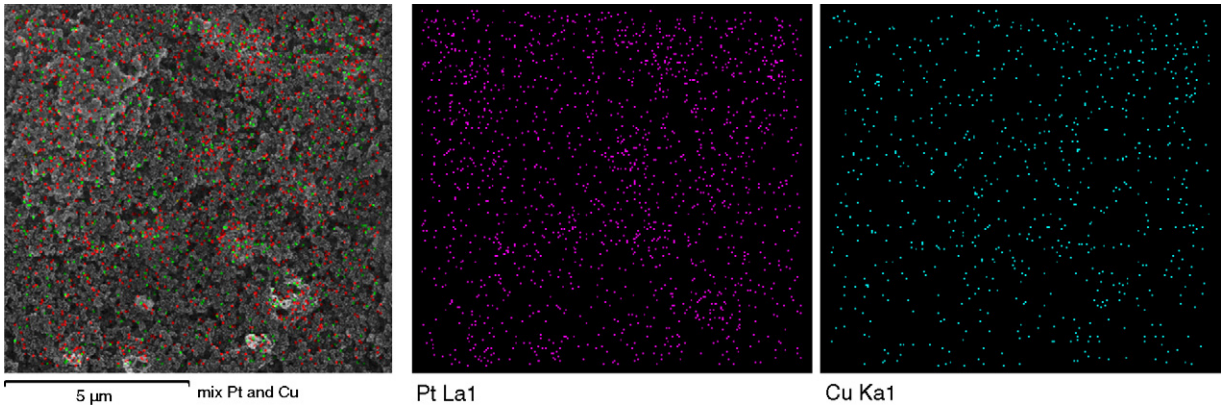

Fig. 7. EDX elemental maps of electrode H.

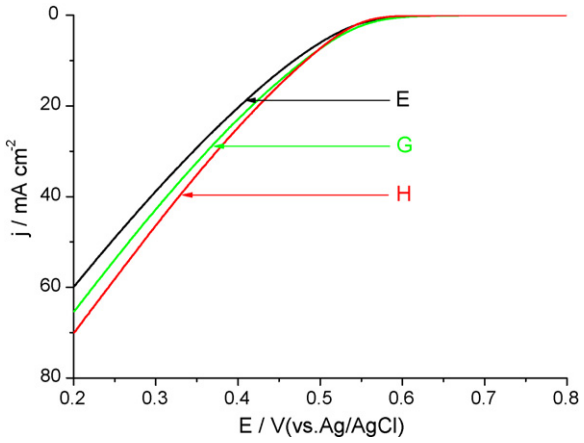

Fig. 8. Performance for the ORR on the electrodes E, G and H.

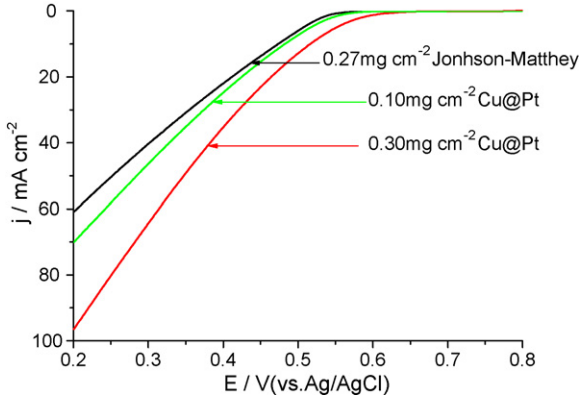

Fig. 9. Performance of the electrodes with Cu/Pt core-shell structured catalysts and commercial Pt/C catalyst for the ORR.

trode. It means that the stability of the Cu/Pt core-shell structured catalyst is reasonably stable. The long-term testing is in progress. It should be noted that the accelerated stability testing conditions adopted in the present work is much more severe than that in the literature [24].

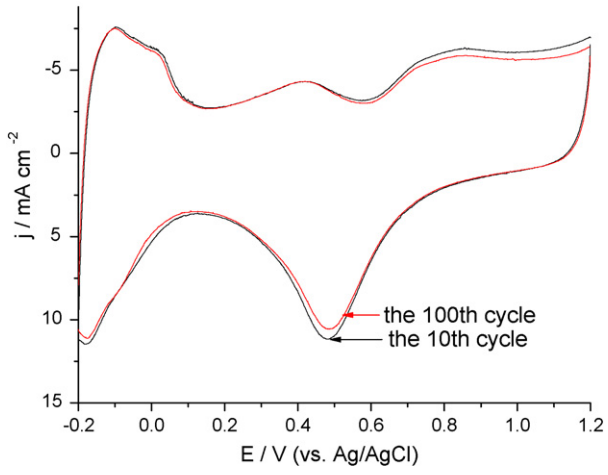

Fig. 10. The 10th and 100th CVs of the electrode with Cu/Pt core-shell structured catalyst at a sweep rate of 50 mV s^{-1} in N_2 saturated 0.5 M H_2SO_4.

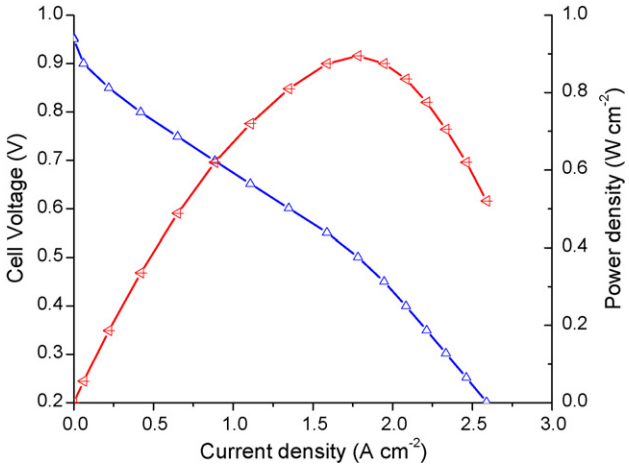

Fig. 11. Cell voltage and power density vs. current density. backpressure: $PO_2 = 200$ kPa, $PH_2 = 200$ kPa; the catalyst loadings are 0.24 mg cm^{-2} Pt for both cathode and anode; $T_{cell} = 70\,^{\circ}C$.

The performance of a single cell using Cu/Pt core-shell structured catalysts is demonstrated in Fig. 11. It is a miracle for a cell to output a power density of 0.9 W cm^{-2} with such a low Pt loadings of 0.24 mg cm^{-2} at each electrode. It further confirms the advantages of the Cu/Pt core-shell structured catalysts prepared by the method invented in this work. That is, it inherits all merits with electrodepositing metal catalyst on the porous electrode, such as selectively depositing metallic catalysts at the sites where metallic catalysts can be fully utilized, gradient depositing across the catalyst layer by controlling the deposition rate [25]. The harassment of hydrogen evolution, which is accompanied with direct Pt deposition, is completely avoided. The excellent results due to the use of Cu/Pt core-shell structured catalysts are encouraging which potentially applicable to commercial electrode fabrication.

4. Conclusions

Cu/Pt nanoparticles with core-shell structure were successfully prepared by two steps of electrodeposition of Cu and partial replacement of deposited Cu by Pt. It found that in the second step, it is necessary to add TU adjust pH to prevent Cu from self-dissolution with dissolved oxygen. The catalytic activities of the electrodes with Cu/Pt core-shell structured catalysts are much better than that of the electrode with commercial Pt/C solid sphere catalyst even though the Pt loadings in the case of Cu/Pt core-shell structured catalysts are lower (0.10 mg cm^{-2} against 0.27 mg cm^{-2}). It demonstrated that the single cell with Cu/Pt core-shell structured catalysts gave better performance for ORR. It is a miracle for a single PEMFC to output a power density of 0.9 W cm^{-2} with Pt loadings as low as 0.24 mg cm^{-2} at each electrode. The excellent results due to the use of Cu/Pt core-shell-like structured catalysts are encouraging which potentially applicable to the fabrication of high performance electrodes for the PEMFCs.

Acknowledgements

This work was financially supported by NSFC of China (Grant No. 20676156), by the Chinese Ministry of Education (Grant No. 307021), China National 863 Program (Grant Nos. 2006AA11A141 and 2007AA05Z124), Chongqing Sci & Tech Key Project (Grant No. CSTC2007AB6012), and Guangdong Sci & Tech Key Projects (Grant Nos. 2007A010700001, 2007B090400032 and 2007Z1-D0051).

References

[1] R. Bashyam, P. Zelenay, Nature 443 (2006) 63–66.
[2] A.J. Dickinson, L.P.L. Carrette, J.A. Collins, K.A. Friedrich, U. Stimming, Electrochim. Acta 47 (2002) 3733–3739.
[3] S. Wasmus, A. Kuver, J. Electroanal. Chem. 461 (1999) 14–31.
[4] S.H. Joo, S.J. Choi, I. Oh, J. Kwak, Z. Liu, O. Terasaki, R. Ryoo, Nature 412 (2001) 169–172.
[5] M. Uchida, Y. Fukuoka, Y. Sugawara, H. Ohara, A. Ohta, J. Electrochem. Soc. 145 (1998) 3708–3713.
[6] S. Hirano, J. Kim, S. Srinivasan, Electrochim. Acta 42 (1997) 1587–1593.
[7] K.H. Choi, H.S. Kim, T.H. Lee, J. Power Sources 75 (1998) 230–235.
[8] J. Lee, J. Seo, K. Han, H. Kim, J. Power Sources 163 (2006) 349–356.
[9] G. Stab, P. Urban, US Patent 6,258,239 (2001).
[10] N. Tian, Z.Y. Zhou, S.G. Sun, Y. Ding, Z.L. Wang, Science 316 (2007) 732–735.
[11] H. Tang, J.H. Chen, Z.P. Huang, D.Z. Wang, Z.F. Ren, L.H. Nie, Y.F. Kuang, S.Z. Yao, Carbon 42 (2004) 191–197.
[12] C. Wang, M. Waje, X. Wang, J.M. Tang, R.C. Haddon, Y.S. Yan, Nano Lett. 4 (2004) 345–348.
[13] Y.Y. Shao, G.P. Yin, J.J. Wang, Y.Z. Gao, P.F. Shi, J. Electrochem. Soc. 153 (2006) 1261–1265.
[14] Z.D. Wei, S.H. Chan, L.L. Li, H.F. Cai, Z.T. Xia, C.X. Sun, Electrochim. Acta 50 (2005) 2279–2287.
[15] Z.D. Wei, S.H. Chan, J. Electroanal. Chem. 569 (2004) 23–33.
[16] L. Yang, J.H. Chen, X.X. Zhong, K.Z. Cui, Y. Xu, Y.F. Kuang, Colloids Surf. A: Physicochem. Eng. Aspects 295 (2007) 21–26.
[17] S.H. Zhou, B. Varughese, B. Eichhorn, G. Jackson, K. McIlwrath, Angew. Chem. Int. Ed. 44 (2005) 4539–4543.
[18] Y.J. Kang, T.A. Taton, Angew. Chem. Int. Ed. 44 (2005) 409–412.
[19] K.H. Ng, R.M. Penner, J. Electroanal. Chem. 522 (2002) 86–94.
[20] H.G. Ling, E.S. Lee, K.B. Kim, Colloids Surf. A: Physicochem. Eng. Aspects 262 (2005) 125–131.
[21] M. Ueda, H. Dietz, A. Anders, H. Kneppe, A. Meixner, W. Plieth, Electrochim. Acta 48 (2002) 377–386.
[22] S.X. Cai, C. Huang, Noble Metal Analysis, 1st ed., Metallurgical Industry Press, Beijing, 1984, pp. 199.
[23] J. Yang, J.Y. Lee, L.X. Chen, H.P. Too, J. Phys. Chem. B 109 (2005) 5468–5472.
[24] J. Zhang, K. Sasaki, E. Sutter, R.R. Adzic, Science 315 (2007) 220–222.
[25] O. Antoine, Y. Bultel, P. Ozil, R. Durand, Electrochim. Acta 45 (2000) 4493–4500.